EXPERIMENTAL RESULTS ON NEUTRINO OSCILLATIONS USING ATMOSPHERIC, SOLAR AND ACCELERATOR BEAMS*

Danuta Kiełczewska

for the SuperKamiokande and K2K Collaborations

Institute for Experimental Physics, Warsaw University
Hoża 69, 00-681 Warsaw, Poland
and Physics Department, University of California
Irvine, CA 92697, USA
e-mail: danka@fuw.edu.pl

The innermost secrets of the mysterious neutrino are being revealed in underground detectors. Recent data on atmospheric neutrinos, primarily from the Super-Kamiokande experiment, confirm the neutrino flavor mixing and non-zero masses. The high precision measurement of angular distribution allows to determine the value of Δm^2 between 0.0013 eV^2 and 0.0054 eV^2 at 90% c.l. Studies of up–down asymmetries in different event samples indicate that $\nu_\mu \leftrightarrow \nu_\tau$ oscillations are more likely explanation of the data than $\nu_\mu \leftrightarrow \nu_s$. The deficit of the observed solar neutrino flux compared to the predictions of the standard solar model, often interpreted by neutrino oscillations, is further studied in the SuperKamiokande detector. The energy spectrum is measured above 5.5 MeV for the Sun's positions above and below the horizon. A day–night effect is observed at a statistical significance of 2 σ. The K2K (KEK to Kamioka) is the first long-baseline neutrino-oscillation experiment. During runs in 1999 the first 3 events were observed in the SuperKamiokande detector caused by neutrinos produced at the KEK accelerator at a distance of 250 km. The predicted number of events without any oscillations is $12.3^{+1.7}_{-1.9}$.

PACS numbers: 14.60.Pq, 14.60.St, 95.55.Vj, 96.40.Tv

---

1. Introduction

Atmospheric neutrinos are produced by cosmic rays in the Earth's upper atmosphere. As a result of a power-law momentum spectrum of primary cosmic rays the neutrinos have mostly energies of a few GeV. They arise mainly from the decay chain $\pi \to \mu\nu_\mu, \mu \to e\nu_\mu \, \nu_e$ and thus at low energies they are composed of muon and electron flavor at a proportion of 2:1.

Predictions of the absolute flux of atmospheric neutrinos [1–3] suffer from fairly large uncertainties of the input ingredients of the calculations, mainly the primary cosmic ray flux and hadronic interactions. However, the ratio of muon to electron flavor content is calculated with an error of less than 5%. The measurements of this ratio over last decade indicated a deficit of muon neutrinos [4–6] but systematic uncertainties in models of neutrino interactions prevented an unique interpretation of the effect. Kamiokande collaboration also observed an angular modulation of the ratio albeit with a small statistics [7].

Much larger samples collected in SuperKamiokande (SK) detector allowed for more robust, model independent evidence for $\nu_\mu \leftrightarrow \nu_x$ oscillations based on the observation of up–down angular asymmetry. The results have been published in [8–10]. Angular distributions have also been studied with different experimental techniques by MACRO [11] and SOUDAN [6] collaborations.

The probability of flavor conversion in a simple two-flavor mixing scheme and for neutrino propagation in vacuum is

$$P_{i \to f} = \sin^2 2\theta \sin \left(\frac{1.27 \Delta m^2 (\mathrm{eV}^2) L(\mathrm{km})}{E_\nu (\mathrm{GeV})} \right) , \qquad (1)$$

where Δm^2 denotes the difference of squares of masses of the states rotated by the angle θ with respect to the weak-interaction states and L is the neutrino pathlength.

The distances traveled by neutrinos from their production point in the atmosphere to a detector range from about 10 km for neutrinos produced directly overhead, to $\sim$13000 km for neutrinos produced at antipodes. The attenuation of the flux of neutrinos passing the Earth is insignificant and so studies of angular distributions allow for sensitive tests of the neutrino oscillation hypothesis.

Atmospheric ν_μ neutrinos can be studied in the energy range from 0.2 GeV up to ~ 100 GeV. However at higher energies only upward-going neutrinos can be separated from the background of cosmic ray muons. Hence the sensitivity range of the ratio L/E_ν extends from about 1 km/GeV for the downward-going few-GeV neutrinos to about 6×10^4 km/GeV for the upward-

going neutrinos of the lowest energies. Consequently the experiments can be sensitive to Δm^2 in the range from 10^{-5} eV^2 to 1 eV^2.

A summary of the results obtained by various experiments as well as the details of the analysis of the 990 day SK sample are given in Sec. 2.

Formula (1) implies that solar neutrinos with much larger L/E_ν ratio allow to probe much smaller range of Δm^2. Moreover a resonant enhancement of oscillations (MSW effect [14]) in dense matter of the solar core makes experiments sensitive to much smaller mixing angles.

Significant deficit of electron neutrinos arriving from the Sun has been reported by four different experiments [15–18]. No Standard Solar Model [19,20] modifications are able to explain the observed event rates. The real time observation of solar ν's in SK offers a possibility to test the $\nu_e \leftrightarrow \nu_x$ oscillation hypothesis in a model-independent way by looking for a distortion of the recoil energy spectrum [21] with respect to the shape expected from the decay

$$^8\text{B} \longrightarrow ^8\text{Be}^* + e^+ + \nu_e.$$

Another effect which could reveal new physics of neutrinos is a possible regeneration of ν_e flux in their passage through the Earth core due to MSW effect. Hence the measurements are done separately during day and night [22]. The updated results of a 825 day sample of solar neutrinos collected in SK will be discussed in Sec. 3.

The K2K experiment [24] is the first long-baseline neutrino-oscillation experiment using an artificial neutrino beam. Almost a pure ν_μ beam from π^+ decays is generated in the KEK 12-GeV/c Proton Synchrotron, and neutrino events are detected in the SuperKamiokande detector 250 km away. The experiment is able to probe the $\nu_\mu \leftrightarrow \nu_x$ oscillation parameters which explain the atmospheric ν anisotropy. The first results are described in Sec. 4.

2. Atmospheric neutrinos

2.1. Detectors

Statistically significant samples of atmospheric neutrinos have been collected in the SuperKamiokande [9,10], MACRO [11] and SOUDAN [6] underground detectors. Their properties are summarized in Table I.

Active elements of the MACRO detector are streamer tube chambers used for tracking and liquid scintillator counters for the time measurements. The lower half of the detector is filled with trays of crushed rock absorber alternating with streamer tube planes, while the upper part is open. The muon direction is determined by the time-of-flight between two out of three existing layers of scintillator counters.

TABLE I

Detectors of atmospheric neutrinos

	SuperKamiokande [9,10]	MACRO [11]	SOUDAN 2 [6]
Location	Japan	Italy Gran Sasso	USA
Technique	water Cherenkov	tracking calorimeter	tracking calorimeter
Depth (m.w.e)	$\gtrsim 2700$	$\gtrsim 2700$	2100
Dimensions	41 m $\times$39 m ϕ	$77 \times 12 \times 9$ m^3	$16 \times 8 \times 6$ m^3
Total mass	50 kt	5.3 kt	0.963 kt
Exposure[a]	61 kt-yr	16.8 kt-yr	4.6 kt-yr
Event samples	contained up-muons	partially cont. up-muons	fully cont.

[a] Exposure is a product of fiducial volume and live time for contained events.

The SOUDAN 2 detector is a fine-grained gas tracking calorimeter consisting of 224 modules. The iron sheets 1.6 mm thick are interleaved with plastic drift tubes of 1.3 cm diameter. The detector is surrounded by active shield to tag events associated with cosmic ray muons passing close to the detector.

The SuperKamiokande experiment is a large water Cherenkov detector located in Mozumi, Japan. Its total mass of ultra-pure water is 50 kton, divided into two concentric cylinders: an inner volume with its inside surface covered by 11146 inward-looking 50 cm photomultiplier tubes, and an outer volume serving as entering particle shield and veto with 1885 outward-looking 20 cm phototubes. The fiducial mass of the inner volume (2 m away from the walls) is 22.5 kton. The data taking started in April 1996.

2.2. Event categories

As a result of a power-law momentum spectrum of primary cosmic rays the neutrinos have mostly energies around 1 GeV. In a large underground detector they give rise to the interactions occurring inside the fiducial volume of the detector, called *contained* events. The events are called fully contained (FC) if charged products do not leave the inner detector volume, otherwise they are classified as partially contained (PC).

The FC events of the SK sample are additionally subdivided into "sub-GeV" (with visible energy <1.33 GeV) and "multi-GeV" (>1.33 GeV) events.

One can significantly increase a chance to study high energy neutrinos taking into account interactions occurring in the rock outside of the detector

with muons entering the detector fiducial volume. Due to the large background of the downward-going cosmic ray muons the neutrino-induced events can be selected only if they produce *upward-going muons*. The upward-going muons can either traverse the entire detector ("through-going") or stop inside of it.

The neutrino energies for different event categories in SuperKamiokande are displayed in Fig. 1. Details of the event selection and reconstruction are described elsewhere [9, 10, 12, 13, 25].
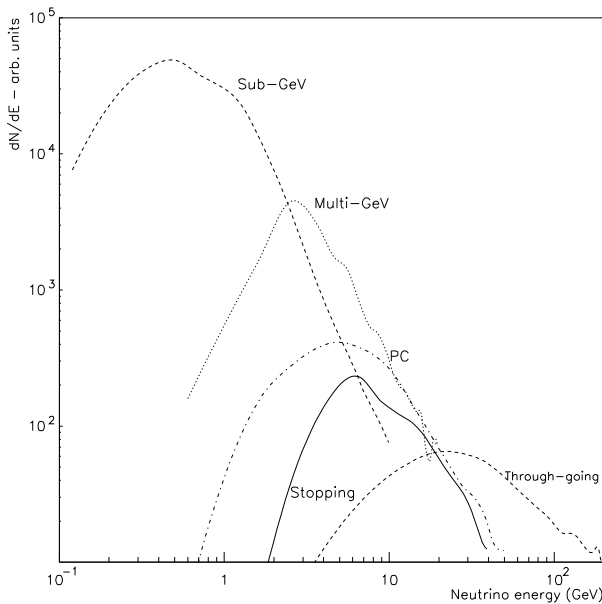
Fig. 1. Energy distribution of parent neutrinos that produce event categories of the SuperKamiokande sample described in the text.

2.3. Contained events

At energies of a few GeVs the neutrino interactions are dominated by quasi-elastic processes $\nu N_1 \to l^{\pm} N_2$ or one pion production $\nu N_1 \to l^{\pm} N_2 \pi$ with low energy pions. It is then possible to determine neutrino flavor on the basis of the charged lepton $l^{\pm}$ flavor. An identification of the latter is possible because electrons develop electromagnetic showers, with subsequent generations of lower energy electrons undergoing a substantial multiple scattering. In the SuperKamiokande and the fine grain SOUDAN 2 detector they can be quite easily separated from the muons.

The measured flavor ratio is conventionally compared to expectation as the "ratio of ratios", R, defined as

$$R = \frac{(N_\mu/N_e)_{\text{DATA}}}{(N_\mu/N_e)_{\text{MC}}}, \qquad (2)$$

where N_μ and N_e are numbers of μ-like and e-like events for data and MC. The μ-like category contains also charged pions, while e-like events include γ's and π^0's. Thus a transformation from R defined above to ratios of the neutrino flavors entails certain model dependence, because a small fraction of events (mostly e-like) are due to neutral current interactions. The resulting uncertainties are included in systematic errors. For no oscillations, R is expected to be 1. However, R is significantly smaller than 1 for a variety of data sets collected in different detectors.

Table II displays statistics available in different categories of contained events recorded in all three detectors. They correspond to the exposures shown in Table I.

TABLE II

Contained events used for studies of the neutrino flavor ratio

| | SuperKamiokande | | | | MACRO | | SOUDAN | |
	Sub-GeV		Multi-GeV					
	Data	MC	Data	MC	Data	MC	Data	MC
Single track:								
e-like	2185	2082	492	481			168	160.6
μ-like	2178	3137	421	640			111	170.5
PC μ-like			563	819	116[a]	202		
R	0.66 ± 0.06		0.66 ± 0.09		0.57 ± 0.16[b]		0.68 ± 0.11	

[a] only upward-going muons
[b] here R is defined as Data/MC

In the MACRO experiment the information from the layers of time-of-flight scintillators determines whether a particle is going up or down and thus only partially contained events are selected. Because the directional information is missing in the SOUDAN data, only the fully contained events are used for the flavor analysis. According to MC simulations 98% of PC events in SuperKamiokande are due to ν_μ charged current interactions. In MACRO about 13% of PC events are due to either neutral currents or ν_e.

2.3.1. Angular distributions of single ring events

At energies relevant for atmospheric neutrinos there is no significant flux attenuation in Earth and so an approximate up–down symmetry is expected. We then compare the experimental and theoretical distributions of zenith angle. In what follows $\cos\Theta = -1$ corresponds to upward-going neutrinos and $\cos\Theta = +1$ corresponds to downward-going. Angular distributions for different event categories are compared with MC simulations in Fig. 2. A deficit of muon neutrinos passing through the Earth is clearly seen, while the observed angular distribution of e-like events agrees in shape with simulations.
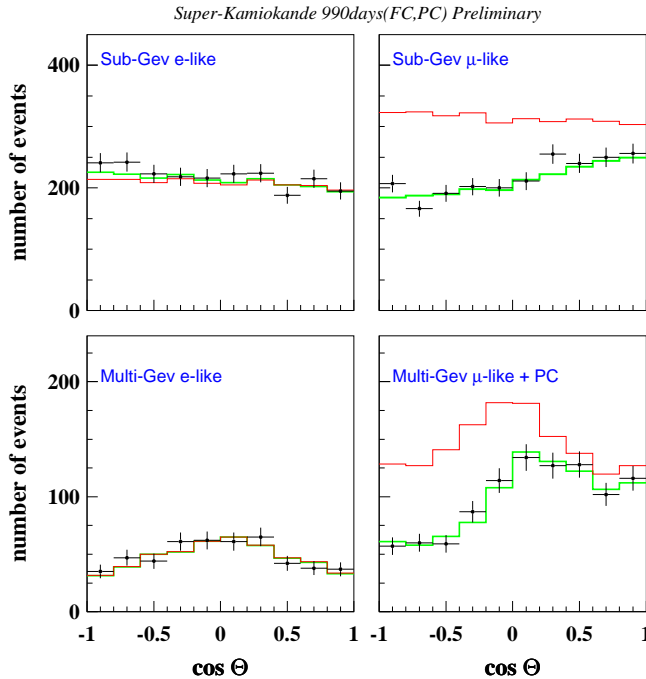
Fig. 2. Preliminary angular distributions for sub-GeV (top) and multi-GeV (bottom) 992 day samples; left figures are for e-like and right for μ-like events. Solid lines show the MC no-oscillation prediction, while broken lines show the $\nu_\mu \leftrightarrow \nu_\tau$ oscillation prediction for the best-fit parameters.

In Fig. 3 an up–down asymmetry $A = \frac{U-D}{U+D}$ is shown as a function of momentum for e-like and μ-like events. The up-going U and down-going D particles are selected with $|\cos\Theta| > 0.2$. For μ-like events the asymmetry is different from zero at a statistical significance of more than 6 σ's.
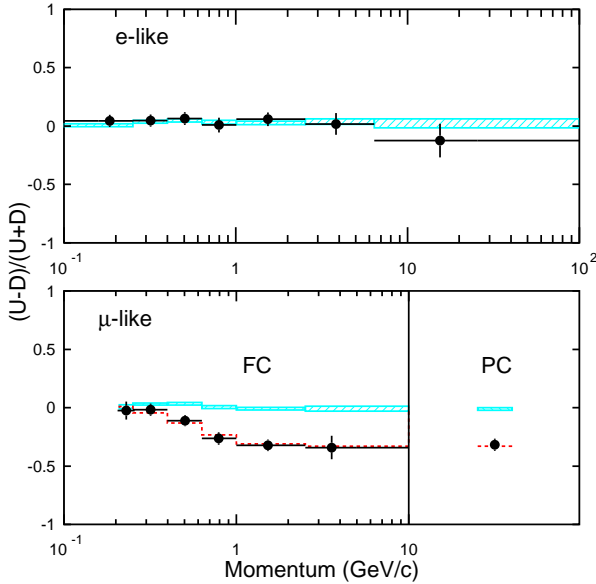
Fig. 3. Up-down asymmetry as a function of momentum for e-like and μ-like events. The boxes display no-oscillation prediction, while the solid lines result from the $\nu_\mu \leftrightarrow \nu_\tau$ oscillations with the best-fit parameters.

The most natural explanation of the asymmetry is offered by the $\nu_\mu \leftrightarrow \nu_\tau$ oscillations, because at the neutrino energies below 10 GeV the charged current (CC) cross-section for ν_τ is significantly smaller than that for ν_μ interactions due to the τ lepton mass.

In order to test the oscillation hypotheses the single ring contained data were divided into 70 bins according to the event energies and directions. A χ^2 was constructed to compare the observed event numbers with those resulted from MC simulations assuming different oscillation parameters. Additional terms in the χ^2 take into account systematic uncertainties. The flux normalization is treated as a free parameter. The details of the procedure are described in [8,28].

Assuming $\nu_\mu \leftrightarrow \nu_\tau$ oscillations the best fit for 992 day sample is obtained for $\sin^2 2\theta = 1.0$ and $\Delta m^2 = 2.6 \times 10^{-3}$ eV^2, with $\chi^2/\mathrm{d.o.f.} = 45/67$, while for no-oscillation hypothesis it is $191/69$, corresponding to a probability of less than 0.0001%. The histograms for the best fit parameters are superimposed in Fig. 2 and 3.

It is interesting to consider also transitions into "sterile" neutrinos which by definition do not interact. The $\nu_\mu \leftrightarrow \nu_s$ oscillations can also reproduce the data [28]. The best fit was obtained for $\sin^2 2\theta = 1.0$ and $\Delta m^2 = 3.3 \times 10^{-3}$ eV^2, with $\chi^2/\mathrm{d.o.f.} = 47/62$.

On the other hand in the two-flavor mixing scheme considered here the sole $\nu_\mu \leftrightarrow \nu_e$ transformation is excluded with $\chi^2/\text{d.o.f.} = 110/67$ ($P < 0.1\%$).

2.3.2. East–west effect

Cosmic rays of a few GeV are deflected by the geomagnetic field thus affecting the neutrino directions. The cutoffs for protons hitting the atmosphere from the east are higher than for the directions from the west. This azimuthal anisotropy is essentially insensitive to the oscillation effects, which depend on neutrino pathlengths determined by zenith but not azimuth angle. Large statistics available in SuperKamiokande make it possible to study this modulation. Events are selected with higher energies when charged lepton directions are well enough correlated with that of the parent neutrinos.

To check the reliability of both the experimental results and the atmospheric neutrino flux calculations, a sample has been selected of nearly horizontal single ring events ($|\cos\Theta| < 0.5$, where Θ is zenith angle) with momentum between 400 and 3000 MeV/c.

Fig. 4 shows the azimuthal distribution for both e-like and μ-like events, along with two flux predictions [1, 3]. The expected deficit from the East is observed. This analysis has been described in detail in Ref. [26] for an earlier sample of data.
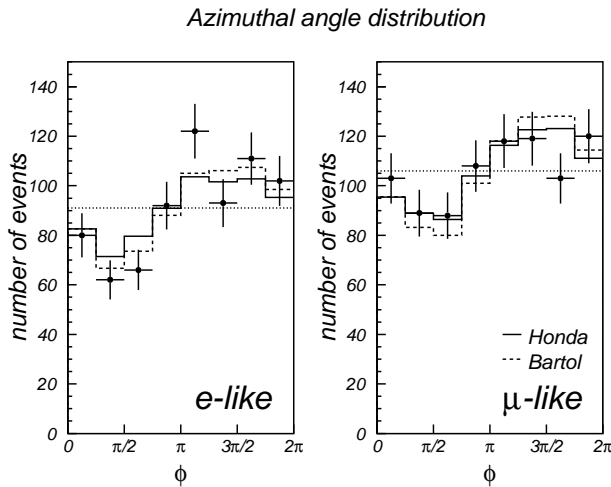

Fig. 4. The East-west effect in SK 992 day sample: azimuthal distribution of nearly horizontal e-like and μ-like events, along with MC predictions based on Honda (solid line) and Bartol (dashed line) fluxes. The angle $\phi = 0$ corresponds to particles going to the north and $\phi = \pi$ corresponds to particles going to the south.

The agreement between the data and calculations provides some evidence that geomagnetic effects are correctly accounted for in the flux predictions. Note also that the Earth magnetic field causes an up–down asymmetry which is confined to energies below 1 GeV and its sign is opposite to the effect displayed by the data in Figs. 2 and 3.

2.4. Upward-going muons

The upward-going muon sample makes it possible to probe higher neutrino energies (*cf.* Fig. 1). With an interaction point outside of the detector the event energy cannot be measured. However a relative rate of stopping to through-going events compared to MC expectations provides an independent information about energy dependence of the oscillations. In the SK 900 day sample the ratio of stopping to through-going muons, $\mathcal{R} = 0.236 \pm 0.018^{+0.013}_{-0.011}$ has been obtained, significantly smaller than the expected $\mathcal{R} = 0.37 \pm 0.05$ for both Bartol and Honda flux calculations.

Available statistics of up-going muons in the SuperKamiokande and MACRO detectors are shown in Table III.

TABLE III

Upward-going muons

	SuperKamiokande			MACRO		
	Live time	Data	MC	Live time	Data	MC
Through-going	2.53 yr	1021	1183	4.5 yr	607	825
Stopping	2.47 yr	228	416	4.1 yr	193[a]	274

[a] The sample includes also partially contained downward-going muons.

In the high energy events the muon direction is very well correlated with that of a parent neutrino. Fig. 5 shows the flux of through-going muons and the relative fraction of stopping upward muons as functions of zenith angle (SK 1050 day sample). They are compared with corresponding MC predictions using the Bartol neutrino fluxes [12].

The χ^2 analysis described above for the contained single-ring sample has been extended to include 15 additional angular bins for upward-going muons. For $\nu_\mu \leftrightarrow \nu_\tau$ oscillation hypothesis this combined analysis provided the best-fit parameters: $\sin^2 2\theta = 1.0$ and $\Delta m^2 = 2.8 \times 10^{-3}$ eV^2, with $\chi^2/\text{d.o.f.} = 61.1/82$. The acceptable oscillation parameters at different confidence levels are delineated by the contours in Fig. 6. More details on the analysis can be found in Ref. [27].
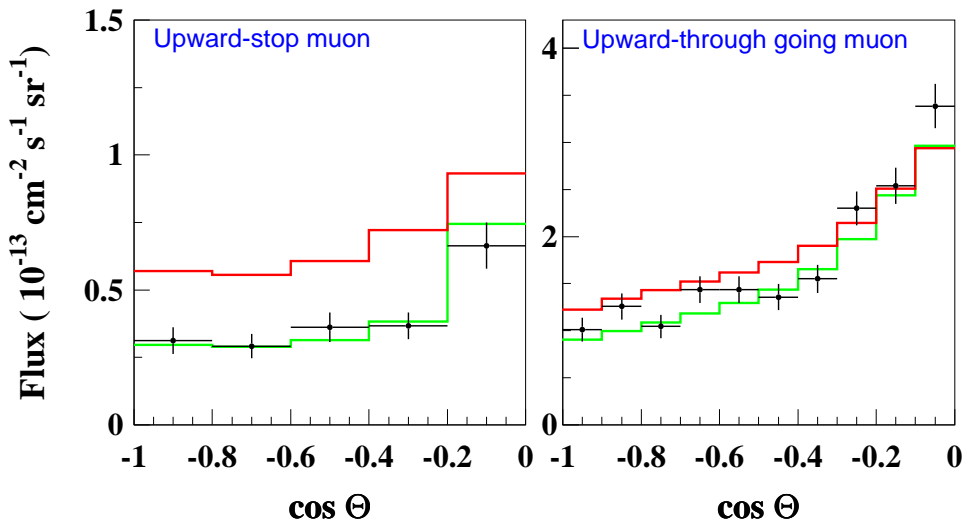
Fig. 5. Zenith angle distribution of SK upward-going muons (1050 day sample): left for stopping events and right for through-going. The data points are compared with the no-oscillation flux predictions (solid lines), and the best fit $\nu_\mu \leftrightarrow \nu_\tau$ oscillations (the dashed lines).
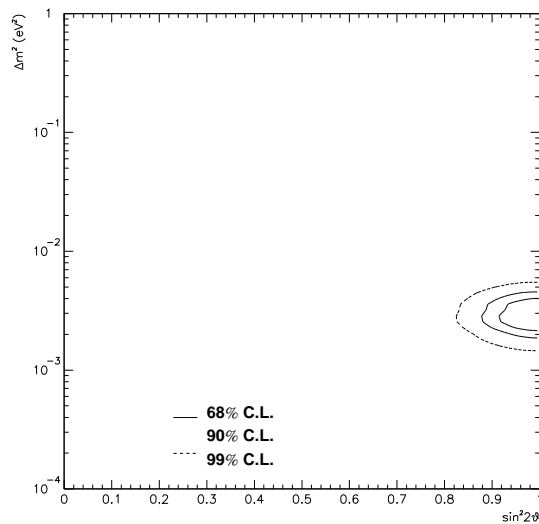

Fig. 6. Allowed regions for parameters of $\nu_\mu \leftrightarrow \nu_\tau$ oscillations using combined information from the contained events and upward-going muons in the SuperKamiokande detector.

Figure 7 compares the precisions with which different experiments can determine the $\nu_\mu \leftrightarrow \nu_\tau$ oscillation parameters. The SK statistics allows to restrict significantly the allowed regions of the parameters which fit the data. It is very reassuring that MACRO and SOUDAN data, which have been collected using different techniques, support the SuperKamiokande result.
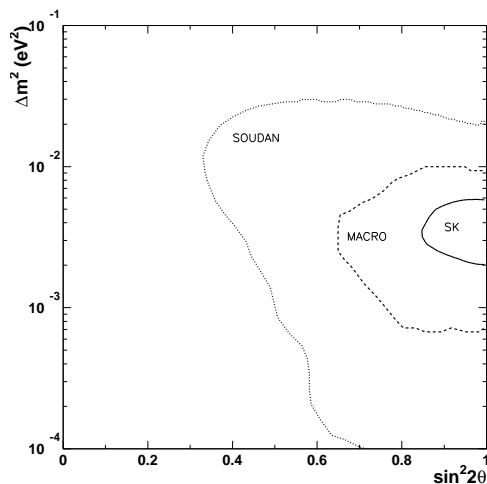

Fig. 7. Parameters of the $\nu_\mu \leftrightarrow \nu_\tau$ oscillations consistent at 90% c.l. with data of SuperKamiokande, MACRO and SOUDAN 2.

2.5. Do muon neutrinos oscillate into ν_τ or ν_s?

The up-down asymmetry of the contained single-track sample (Fig. 3) can be well reproduced by both $\nu_\mu \leftrightarrow \nu_\tau$ and $\nu_\mu \leftrightarrow \nu_s$ oscillations. In order to discriminate between those two hypotheses the following two approaches are possible.

First one can try to select a sample of neutral current (NC) interactions. The $\nu_\mu \leftrightarrow \nu_\tau$ transition would not cause any change in this sample because the NC cross sections are the same for ν_τ and for ν_μ. On the other hand the sterile neutrinos by definition do not interact by the known electro-weak processes and therefore one would expect a reduced rate of NC events in case of $\nu_\mu \leftrightarrow \nu_s$ oscillations. However, a selection of a pure NC sample is generally difficult in a water Cherenkov detector. One channel which is experimentally feasible is $\nu N \to \nu N \pi^0$. However, the cross section for this channel is known too poorly at this stage to make this approach effective.

In order to avoid problems with cross sections one should study an up–down asymmetry. On the basis of a simulated sample a set of cuts has been

determined which enhances a contribution of NC interactions among multi-ring events of the SK data. Figure 8 displays the zenith angle distribution for a sample which consists of 44% of ν_e CC, 27% of ν_μ CC, 7.4% of ν_e NC and 21.3% of ν_μ NC interactions. The data are compared with expectations for both $\nu_\mu \leftrightarrow \nu_\tau$ and $\nu_\mu \leftrightarrow \nu_s$. It is seen that the $\nu_\mu \leftrightarrow \nu_\tau$ oscillations fit better the data.
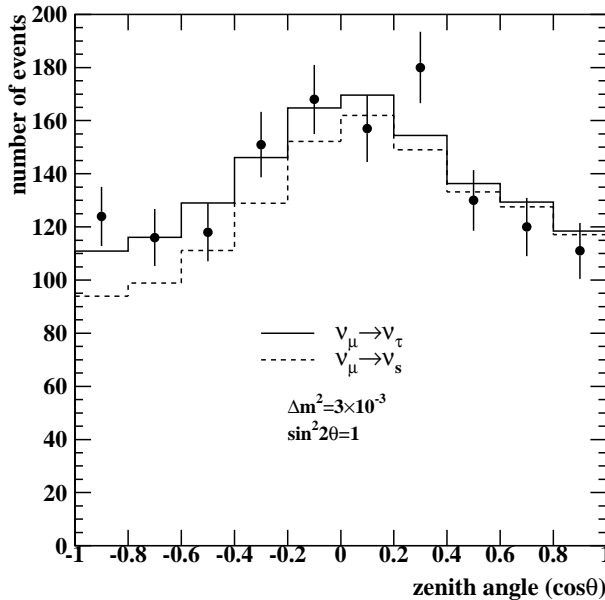

Fig. 8. Zenith angle distribution for a SK multi-ring sample enriched in neutral current interactions. The histograms correspond to $\nu_\mu \leftrightarrow \nu_\tau$ (solid) and $\nu_\mu \leftrightarrow \nu_s$ (dashed) oscillations with the mixing parameters indicated in the figure.

Another approach is to select a sample of charge current interactions in the detector and exploit the matter effects in Earth [14]. During the neutrino passage through Earth the ν_μ and ν_τ undergoes a "refraction" because of the NC interactions with matter. The effect is the same for both flavors. On the other hand the difference in interactions for ν_μ and ν_s leads to a potential term in the difference of energies of propagating neutrinos and consequently to different velocities. An "effective mixing" in matter is then described by:

$$\sin^2 2\theta_m = \frac{\sin^2 2\theta}{\left(\frac{2VE_\nu}{\Delta m^2} - \cos 2\theta\right)^2 + \sin^2 2\theta}, \tag{3}$$

where Δm^2 and θ are the "vacuum" oscillation parameters of formula (1), and V accounts for the interaction difference.

The effect is thus stronger for higher neutrino energies and therefore samples of PC events and upward-going muons are more suitable for this study. The zenith angle distributions for both samples are displayed in Fig. 9, where the data are compared with expectations for both $\nu_\mu \leftrightarrow \nu_\tau$ and $\nu_\mu \leftrightarrow \nu_s$. The statistics are very limited but one can see that ν_s hypothesis is again less likely.
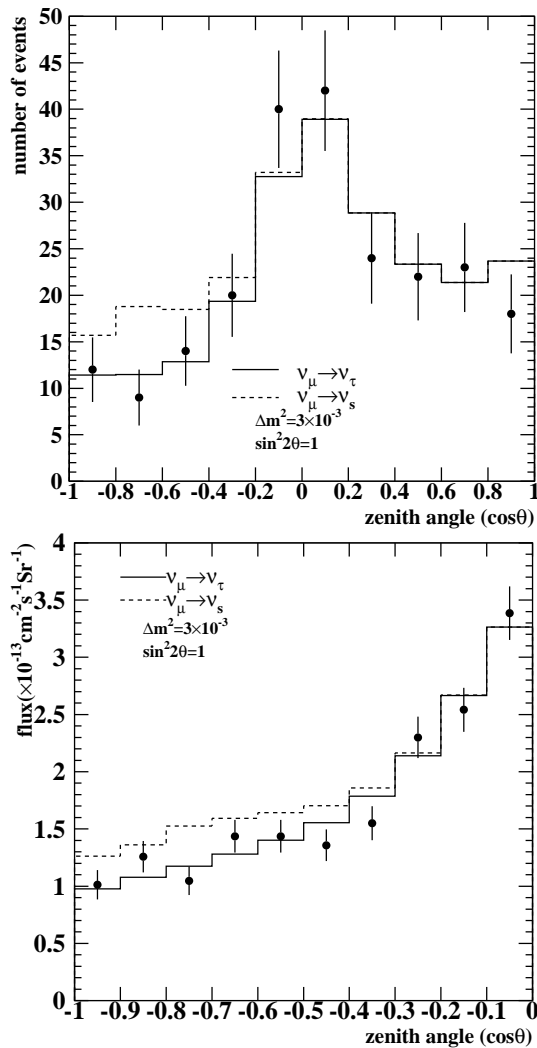

Fig. 9. Zenith angle distributions for PC sample (top) and for upward-going muons (bottom). The histograms correspond to $\nu_\mu \leftrightarrow \nu_\tau$ (solid) and $\nu_\mu \leftrightarrow \nu_s$ (dashed) oscillations with the mixing parameters indicated in the figure.

One can combine the results from the three independent data samples in order to find out the confidence levels for different mixing parameters. They are shown in Fig. 10.
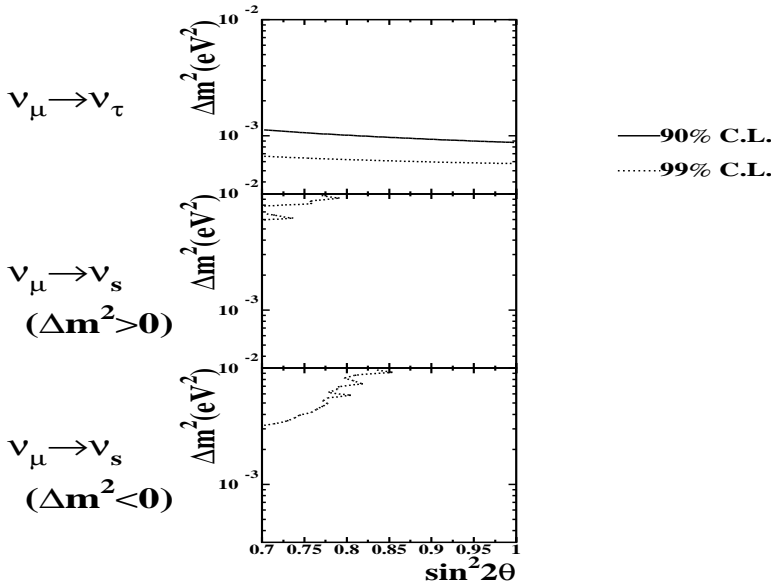

Fig. 10. Excluded regions of the oscillation parameters using combined SK information from the NC enhanced multi-ring sample, PC and upward-going muons, taking into account matter effects [14, 27].

It is seen that the $\nu_\mu \leftrightarrow \nu_s$ oscillation parameters, which could have provided a competitive explanation for the up-down asymmetry observed in the single track contained sample, are excluded by other SK samples. The details of the analysis are described in Ref. [27].

3. Solar neutrinos

Solar neutrinos are observed in SuperKamiokande via elastic neutrino-electron scattering in water:

$$\nu_e + e^- \longrightarrow \nu_e + e^- . \tag{4}$$

Due to kinematics of the reaction the electron follows the neutrino direction. Therefore the angle $\theta_\odot$ between reconstructed electron direction and the current direction away from the Sun can be used to separate solar neutrino interactions from background events (see Fig. 11).

As a result of the analysis of 825 days of data $11235^{+180}_{-166}(\text{stat.})^{+315}_{-303}(\text{syst.})$ signal events above 6.5 MeV recoil electron energy were selected. Assuming
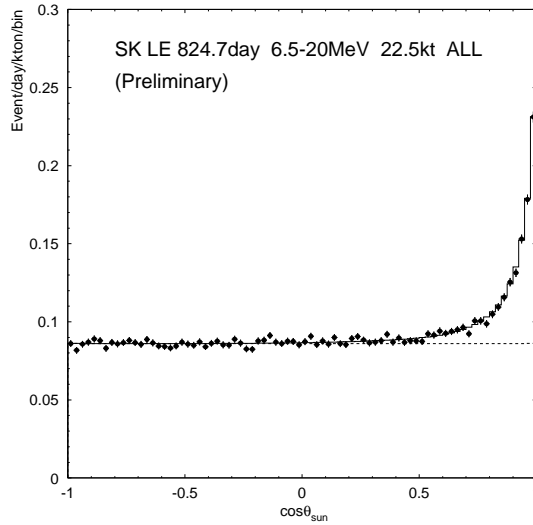
Fig. 11. Angular distribution of electrons with respect to the direction of the Sun. The 'solar peak' at $\cos\theta_\odot = 1$ above the background is used to measure the solar ^{8}B neutrino flux and spectrum.

the ^{8}B spectrum shape the flux is $(2.45\pm0.04(\text{stat.})\pm0.07(\text{syst.}))\times10^6/\text{cm}^2/\text{sec}$. It is significantly lower than expected from the BP98 [19] Standard Solar Model (SSM). The ratio is $\frac{\text{Data}}{\text{SSM}_{\text{BP98}}} = 0.475^{+0.008}_{-0.007}(\text{stat.}) \pm 0.013(\text{syst.})$.

The discrepancy between SSM and the flux measurement may be explained by oscillation of electron neutrinos $\nu_e \leftrightarrow \nu_x$ into another neutrino type, which interacts in the detector with much smaller cross section. In particular muon and tau neutrinos of a few MeV scatter on electrons only via NC and hence their detection rate is much smaller. Another possibility is an oscillation into a sterile neutrino.

If the Δm^2 between dominant components of ν_e and ν_x is very small ($< 10^{-9}\text{eV}^2$) then the flavor conversion occurs in "vacuum", when ν_e travels from the Sun to Earth. If Δm^2 is larger, then the MSW resonant enhancement causes a flavor transformation in the dense solar matter.

SuperKamiokande allows to look for a definite evidence of the oscillation hypothesis, in a model-independent way. In particular any difference between day and night fluxes, unexpected seasonal flux variation or a modulation of electron energy spectrum would provide a more convincing proof of a new neutrino physics.

3.1. Day–night effect

If the MSW effect in the solar matter is responsible for a $\nu_e \to \nu_x$ transition, then for a range of oscillation parameters the $\nu_x \to \nu_e$ process may occur in the Earth, leading to a regeneration of the electron neutrinos and an increase of the signal during nights.

The measured day–night asymmetry is:

$$\frac{2(\mathrm{day} - \mathrm{night})}{\mathrm{day} + \mathrm{night}} = -0.065 \pm 0.031(\mathrm{stat.}) \pm 0.013(\mathrm{syst.})$$

i.e. an effect of 2σ statistical significance. The event rate distribution as a function of the zenith angle of the current Sun position is presented in Fig. 12.

Constraints on neutrino oscillation parameters resulting from the observation are discussed in [17,22].
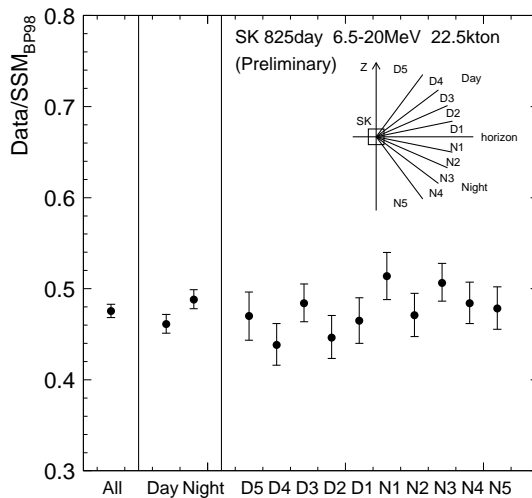

Fig. 12. Normalized neutrino rate as a function of the zenith angle of the Sun's position. The bins are defined in the figure.

3.2. Solar neutrino spectrum

Although the SuperKamiokande measures the energy spectrum of recoil electrons, its shape directly reflects the shape of the spectrum of incoming neutrinos (*cf.* reaction 4). Precision energy calibration have been done [21] with various sources, in particular using an electron linear accelerator providing a tunable energy ranging from 5 to 16 MeV. The uncertainty in the energy scale is estimated to be $\pm 0.8\%$, while the energy resolution is better than 2%.

The event rates are determined in 0.5 MeV energy bins using for each bin the distributions of $\theta_\odot$ and extracting a solar peak as in Fig. 11. Below 6.5 MeV a background due to radioactive impurities increases sharply with decreasing energy. A new Super Low Energy (SLE) analysis was designed to reject these backgrounds more efficiently. Currently, the SLE analysis threshold is at 5.5 MeV.

A convenient way to search for spectral distortions is to divide the observed spectrum by the energy spectrum of simulated electrons based on the SSM BP98 neutrino flux expectations (see Fig. 13). Thus the experimental energy resolution is taken into account. The uncertainties at the end of the spectrum are dominated by limited statistics. The χ^2 for a flat normalized distribution is 24.3/17, corresponding to 11% c.l.
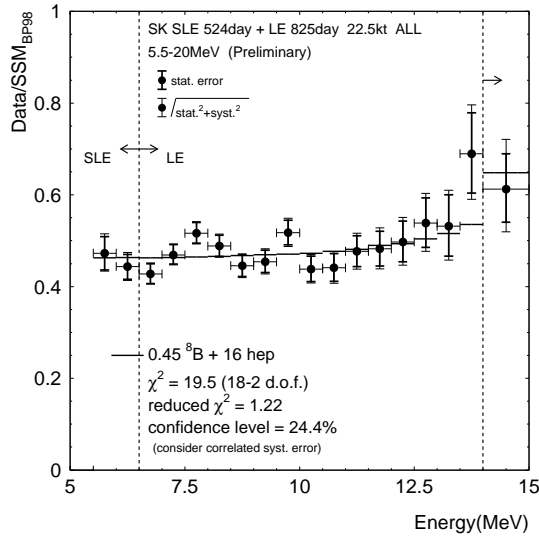

Fig. 13. The recoil electron spectrum measured by SK and normalized to the SSM expectations. The histogram is for the best no oscillation fit without constraint on the ^{8}B or Hep flux normalization.

However the observed relative increase in the flux at the end of the spectrum can also be explained [29] by much higher than expected flux of "Hep" neutrinos resulting from the process:

$$^3\mathrm{He} + p \longrightarrow {}^4\mathrm{He} + e^+ + \nu_e \, .$$
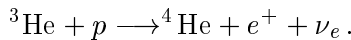
According to the SSM Hep neutrinos contribution is very small but its flux is highly uncertain and extends to 18.8 MeV. Therefore a fit was done to the spectrum shape with relative contribution of Hep flux as a free parameter. As shown in the figure an increase in the Hep flux of a factor of 16 with respect to the SSM fits best the data.

Clearly more data are needed to solve the puzzle at the end of the spectrum. The uncertainty of the Hep flux does not affect lower energies. Therefore a large effort is now undertaken towards decreasing the threshold down to 5 or even 4.5 MeV.

A flux independent oscillation analysis of the day and night spectra has been performed by SK collaboration. The applied χ^2 formalism is similar to the one described in Sec. 2.3.1 and takes into account various systematic errors. The details can be found in Ref. [17]. Table IV contains a few values of χ^2 for parameter regions which best reproduce the flux data of all the experiments.

TABLE IV

χ^2 values from the SK day–night spectrum analysis

Solution	Δm^2 eV^2	$\sin^2 2\theta$	χ^2 SSM Hep 35 d.o.f.	χ^2 Hep free 34 d.o.f.
LMA	3.2×10^{-5}	0.8	47.3	42.2
LOW	2.4×10^{-7}	1.0	47.5	42.0
SMA	5×10^{-6}	0.005	53.3	51.2
VO	4.3×10^{-10}	0.79	44.1	44.2
no oscil.			51.4	46.2

3.3. Seasonal variation

Since the distance from the Sun to Earth changes with a yearly cycle, vacuum oscillations can cause a seasonal modulation of the neutrino flux on top of the conventional r^{-2} flux dependence (indicated with a solid line in Fig. 14). Interestingly, it has been pointed out in Ref. [30] that also MSW oscillations can cause a seasonal flux modulation, if a significant ν_e regeneration occurs in the Earth, which obviously depends on how much time the Sun is under horizon.
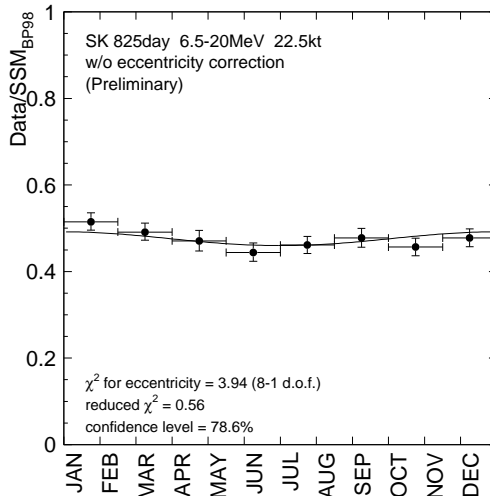
Fig. 14. The seasonal variation for the flux above 6.5 MeV. The line accounts for the variation expected from the Earth orbit eccentricity.

4. K2K — the first long-baseline accelerator experiment

The K2K (for KEK to Kamioka) experiment uses a low-energy neutrino beam produced at the KEK PS accelerator and 2 detector installations: a set of front detectors to monitor the beam and the SuperKamiokande to study the effects of oscillation 250 km away. The $\nu_\mu \leftrightarrow \nu_x$ oscillation can be examined by a ν_μ disappearance because the energy of the neutrino beam is smaller than the τ production threshold. The experiment sensitivity depends then on a precise determination of the original neutrino flux as well as on the measurement of an energy spectrum modulation.

The first data obtained in 1999 runs are described in Ref. [23]. Here we briefly summarize the experiment design and the data.

4.1. Neutrino beam and detectors

The proton beam from the KEK synchrotron produces pions which are focused into a decay channel by a pair of horn magnets (collector and reflector). The momentum and angular distribution of pions is measured by a pion monitor (ring imaging gas Cherenkov counter). Most of the muons from $\pi^+ \to \nu_\mu \mu^+$ decays are stopped in the beam dump. A summary of the proton and neutrino beam properties are given in Table V. The beam is directed 1° downward towards the SuperKamiokande with an accuracy of 1 mrad. Because the absolute flux and energy spectrum of the neutrino beam are expected to be almost constant within 3 mrad, the adjustment of the neutrino beam direction is sufficient.

TABLE V

Properties of the proton and neutrino KEK beams

proton momentum	12 GeV/c
proton intensity	5.4 $\times 10^{12}$ protons/pulse
extraction mode	fast extraction
beam pulse duration	~ 1.1 μsec for every 2.2 sec
target	3cm$\phi \times$ 65cm aluminum
decay tunnel length	200 m
mean ν_μ energy	1.4 GeV
peak ν_μ energy	1.0 GeV
ν_e/ν_μ	$\sim 1\%$
flux at 300m downstream	1.7 $\times 10^{12}\nu$/cm^2 for 10^{20} p.o.t
flux at 250km downstream	1.3 $\times 10^6\nu$/cm^2 for 10^{20} p.o.t

According to MC simulations the beam width at front detectors is about 4 m while it spreads out to 4 km at the SK distance.

The front detector situated 300 m downstream from the target includes a 1 kt water Cherenkov detector (1 kt) and a fine-grained detector (FGD), which in turn consists of the scintillating fiber detector (SFT) [34], scintillation counters, a lead-glass counter and a muon range detector. A schematic view of the K2K front detector is shown in Fig. 15.
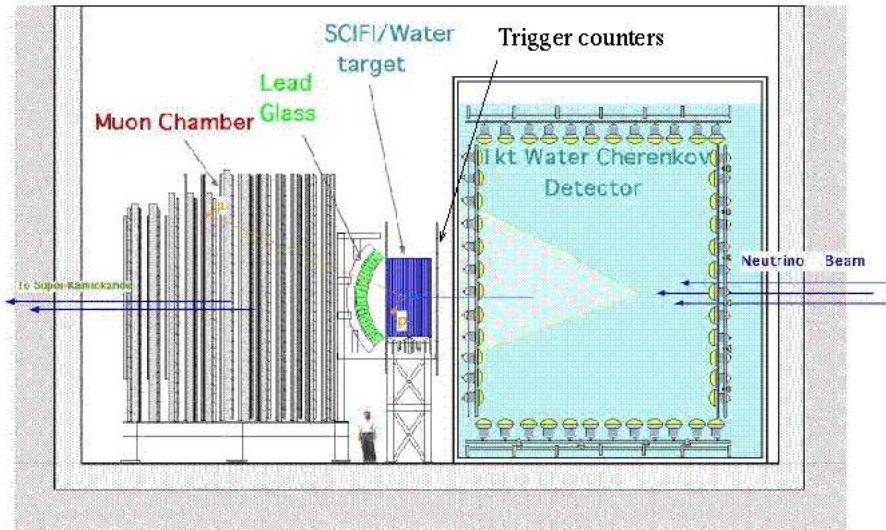

Fig. 15. Front detector in the K2K experiment

4.2. Event rates

The K2K experiment was successfully started in early 1999. A total intensity of 7.20×10^{18} protons on target, which is about 7% of the goal of the experiment, was accumulated in 39.4 days of data-taking in 1999.

The selection of neutrino events in SK is based on the time difference between the neutrino beam spill and each event. Taking into account the neutrino pulse duration (1.1μsec) and accuracy of the absolute time determination ($< 0.3\,\mu$sec), events within a $1.5\,\mu$sec time window covering the neutrino beam period are selected. A total of 12 events have been found, which includes 3 interactions in fiducial volume (FV) of the inner detector. The remaining events occurred either outside of FV or in the outer detector. Because the expected atmospheric neutrino background in FV within the integrated neutrino beam time of 1.5 sec is only 2×10^{-4} events, the three events consist a clear signal of neutrinos from KEK.

The expected event rates in SK ($N_{\mathrm{exp}}^{\mathrm{SK}}$) are obtained from MC simulations rescaled by the observed event rates $N_{\mathrm{obs}}^{\mathrm{FD}}$ in the front detectors:

$$N_{\mathrm{exp}}^{\mathrm{SK}} = \frac{N_{\mathrm{obs}}^{\mathrm{FD}} \times N_{\mathrm{cal}}^{\mathrm{SK}}}{N_{\mathrm{cal}}^{\mathrm{FD}}},$$

where $N_{\mathrm{cal}}^{\mathrm{SK}}$ and $N_{\mathrm{cal}}^{\mathrm{FD}}$ are the calculated event numbers in SK and the front detectors, respectively, using the same simulation program.

The results are summarized in Table VI. It is seen that the scaling ratio $N_{\mathrm{obs}}^{\mathrm{FD}}/N_{\mathrm{cal}}^{\mathrm{FD}}$ is found to be $0.84 \sim 0.85$ consistently for three independent observations.

TABLE VI

Summary of event rates in front detectors

Detector	Fiducial mass (ton)	Number of events	$N_{\mathrm{obs}}^{\mathrm{FD}}/N_{\mathrm{cal}}^{\mathrm{FD}}$
1kt water Cherenkov	50.3	17672	0.84 ± 0.08
Scintillating fiber tracker	5.94	662	$0.85^{+0.08}_{-0.09}$
Muon chamber	445	56062	0.85 ± 0.11

The expected number of events in SK is then $12.3^{+1.7}_{-1.9}$ in 22.5 ktons of FV, and $\sim$31 events in the total volume. Although the observed event rates are considerably smaller than the expectations, more statistics are needed for definitive statements.

4.3. Energy spectrum

To determine the neutrino energy spectrum, quasi-elastic interactions, $\nu_\mu N \rightarrow \mu N'$, in the scintillating fiber tracker are used. This sample is selected because most of the neutrino energy is transferred to the muons and the muon energy can be measured from the range in the muon chamber. The neutrino energy can be directly calculated from the muon energy with a small correction related to the scattering angle of the muon. It should also be noted that quasi-elastic scatterings are detected as single ring events in SK, and can be easily analyzed.

The muon energy distribution for quasi-elastic interactions in the scintillating fiber tracker is shown in figure 16(a) along with expectations from a MC simulation. For a comparison, the expected neutrino energy spectrum in SK is shown in figure 16(b), together with the spectrum for two sets of oscillation parameters, $\Delta m^2 = 0.01\,\mathrm{eV}^2$ and $\Delta m^2 = 0.005\,\mathrm{eV}^2$.
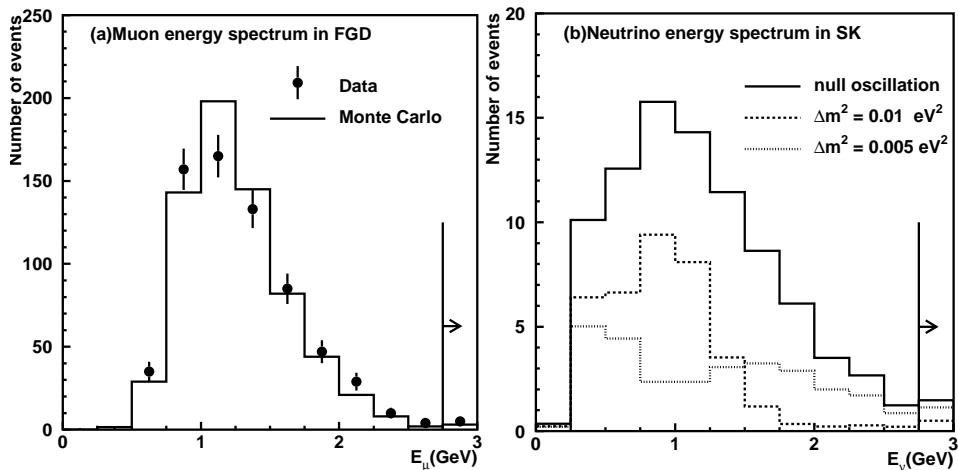

Fig. 16. (a) Muon energy spectrum obtained from the fine-grained detector, compared with MC simulations (histogram). (b) Expected neutrino energy spectrum at SK. The dashed line is for $\Delta m^2 = 0.01\,\mathrm{eV}^2$ and $\sin^2 2\theta = 1$, while the dotted line for $\Delta m^2 = 0.005\,\mathrm{eV}^2$ and $\sin^2 2\theta = 1$.

4.4. Future prospects

From January 2000 to March 2001, about 160 days of data taking are scheduled. If the data can be accumulated with 100% efficiency, we will obtain a total intensity of 46×10^{18} p.o.t., and about 70 events should be observed by the end of March 2001.

The sensitive region of the neutrino oscillation parameters for $\nu_\mu \leftrightarrow \nu_\tau$ oscillations is shown in figure 17 for an assumed integrated ν beam corresponding to 10^{20} p.o.t. It takes into account the recent progress in the simulation of neutrino beam, neutrino interactions, and the detector response.
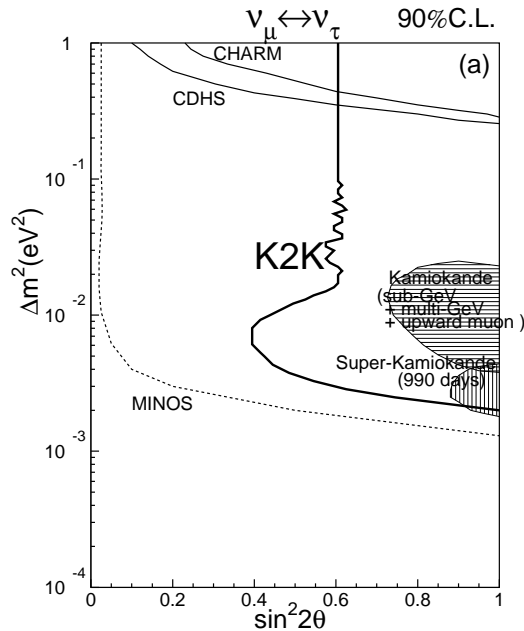

Fig. 17. K2K sensitive region of the neutrino oscillation parameters, Δm^2 and $\sin^2 2\theta$ for $\nu_\mu \leftrightarrow \nu_\tau$ oscillation. The allowed region by Kamiokande and SuperKamiokande as well as excluded (or sensitive) regions by other experiments are also plotted in solid (dashed) lines.

5. Summary

Precise measurements of angular distributions of atmospheric neutrinos in the SuperKamiokande detector provide a clear evidence for muon neutrino oscillations. They imply that neutrinos are massive (at least one ν mass is larger than 0.04 eV) and the Standard Model needs to be extended. This opens many areas of investigations which should indicate the roads for the extension.

The best interpretations of data is obtained for $\nu_\mu \leftrightarrow \nu_\tau$ flavor transformation with maximal mixing and a $(mass)^2$ difference of 0.0013 eV^2 to 0.0054 eV^2. The evidence comes from the sample of contained single ring

events, but is confirmed by upward-going muon sample. The evidence and the oscillation parameters are supported by the results obtained with different experimental techniques by MACRO and SOUDAN collaborations.

Recent SK analysis of the PC and upward-going muon events have shown that $\nu_\mu \leftrightarrow \nu_s$ oscillations do not reproduce the data as well as $\nu_\mu \leftrightarrow \nu_\tau$. Additional information can be expected in the future from a sample of NC interactions: $\nu_l\ N \rightarrow \nu_l\ \pi^0\ N'$, because the K2K experiment gives a chance to improve our knowledge of pion production in water in order to reduce systematic errors.

The real time nature of the SK solar ν measurements offers a possibility to study the $\nu_e \leftrightarrow \nu_x$ oscillation hypothesis in a model independent way. The day–night asymmetry was found different from zero at $2\ \sigma$ level. The energy spectrum measurements are also inconclusive. The solar neutrino puzzle has been complicated by a large uncertainty in the Hep neutrino flux, which underlines the necessity for still more precise measurements of the ^{8}B neutrino spectrum, especially at the lowest energies.

The near future should abound in data from new detectors. The Sudbury Neutrino Observatory (SNO) [31] has already started to collect the data on ^{8}B neutrinos. It aims to measure a NC signal, which would give a definite evidence of the oscillations. In 2001 Borexino [32] and KamLAND [33] should be operational. Borexino will hopefully measure the solar ν spectrum down to 250 keV and KamLAND studies of reactor antineutrinos should be sensitive to large mixing at $\Delta m^2 > 10^{-5}$ eV^2.

Several long-baseline experiments are dedicated to investigate the $\nu_\mu \leftrightarrow \nu_x$ oscillations observed in atmospheric neutrinos, using the accelerator beams. The K2K experiment, the first of the series, has already collected valuable experience and the first data. It will run for a few more years, but it's likely that it will provide an independent confirmation of oscillations within this year. The MINOS experiment [35] using the Fermilab intense ν_μ beam will be operational in 2003, while in 2005 the CERN long-baseline neutrino program should start. The ν_μ beam will be directed from CERN to Gran Sasso, where 2 detectors: ICANOE [36] and OPERA [37] are designed to observe ν_τ appearance.

We can expect to know the full neutrino mixing and mass matrices in a foreseeable future. Moreover, we can hope that mysterious neutrinos will surprise us with more of secrets of nature to reveal.

REFERENCES

[1] M. Honda *et al.*, *Phys. Lett.* **B248**, 193 (1990); *Phys. Rev.* **D52**, 4985 (1995); *Prog. Theor. Phys. Suppl.* **123**, 483 (1996).

[2] G. Barr *et al.*, *Phys. Rev.* **D39**, 3532 (1989); V. Agrawal *et al.*, *Phys. Rev.* **D53**, 1313 (1996); T.K. Gaisser, T. Stanev, Proc. 24th Int. Cosmic Ray Conf. (Rome) Vol. 1, 694 (1995); T.K. Gaisser, The 18th Int. Conf. on Neutrino Physics and Astrophysics, NEUTRINO 98, Takayama, 1998. *Nucl. Phys. B (Proc. Suppl)* **B77**, 133 (1999).

[3] P. Lipari, T.K. Gaisser, T. Stanev, *Phys. Rev.* **D58**, 073003 (1998).

[4] T.J. Haines *et al.*, *Phys. Rev. Lett.* **57**, 1986 (1986); D. Casper *et al.*, *Phys. Rev. Lett.* **66**, 2561 (1991); R. Becker-Szendy *et al.*, *Phys. Rev.* **D46**, 3720 (1992).

[5] K.S. Hirata *et al.*, *Phys. Lett.* **B205**, 416 (1988); K.S. Hirata *et al.*, *Phys. Lett.* **B280**, 146 (1992).

[6] W.W.M. Allison *et al.*, *Phys. Lett.* **B391**, 491 (1997); T. Kafka, Proceed. of TAUP99 Conf., Paris, Sep. 6–10, 1999; W.W.M. Allison *et al. Phys. Lett.* **B449**, 137 (1999).

[7] Y. Fukuda *et al.*, *Phys. Lett.* **B335**, 237 (1994).

[8] Y. Fukuda *et al.*, *Phys. Rev. Lett.* **81**, 1562 (1998).

[9] Y. Fukuda *et al.*, *Phys. Lett.* **B433**, 9 (1998).

[10] Y. Fukuda *et al.*, *Phys. Lett.* **B436**, 33 (1998).

[11] S. Ahlen *et al.*, *Nucl. Instrum. Methods* **A324**, 337 (1993); M. Ambrosio *et al.*, *Astropart. Phys.* **9**, 105 (1998); F. Ronga, Proceed. of TAUP99 Conf., Paris, Sep.1999, `hep-ex/0001058`.

[12] Y. Fukuda *et al.*, *Phys. Rev. Lett.* **82**, 2644 (1999).

[13] Y. Fukuda *et al.*, *Phys. Lett.* **B467**, 185 (1999).

[14] S.P. Mikheev, A.Y. Smirnov, *Sov. J. Nucl. Phys.* **42**, 913 (1985); *Nuovo Cimento* **9C**, 17 (1986); L. Wolfenstein, *Phys. Rev.* **D17**, 2369 (1978).

[15] J.N. Bahcall, *Neutrino Astrophysics*, ed. Cambridge University Press, 1989.

[16] Y. Fukuda *et al.*, *Phys. Rev. Lett.* **81**, 1158 (1998).

[17] Y. Suzuki, Proceedings on Lepton-Photon Symposium, 1999.

[18] J.N. Bahcall, R. Davis, Jr., *PASP* **112**, 429 (2000).

[19] J. Bahcall, S. Basu, M. Pinsonneault, *Phys. Lett.* **B433**, 1 (1998).

[20] A.S. Brun, S. Turck-Chieze, P. Morel, *Astrophys. J.* **506**, 913 (1998).

[21] Y. Fukuda *et al.*, *Phys. Rev. Lett.* **82**, 2430 (1999); M. Nakahata *et al.*, *Nucl. Instrum. Methods* **A421**, 113 (1999).

[22] Y. Fukuda *et al.*, *Phys. Rev. Lett.* **82**, 1810 (1999).

[23] Y. Oyama for the K2K Collaboration, talk at XXXVth Rencontres de Moriond "Electroweak interactions and unified theories", Les Arcs, Savoie, France, March 11-18, 2000, `hep-ex/0004015`.

[24] K. Nishikawa *et al.*, KEK-PS proposal, *Nucl. Phys. (Proc. Suppl.)* **B59**, 289 (1997); Y. Oyama, talk at the YITP Workshop on Flavor Physics, Kyoto, January, 1998, `hep-ex/9803014 (1998)`.

[25] K. Scholberg for the Super-Kamioande Collaboration, talk presented at 8th International Workshop on Neutrino Telescopes, Venice, February 23–26, 1999, `hep-ex/9905016`.

[26] T. Futagami *et al.*, *Phys. Rev. Lett.* **82**, 5194 (1999).

[27] K. Ishihara, PhD Thesis, University of Tokyo, Dec. 1999.

[28] M.D. Messier, PhD thesis, Boston University, 1999.

[29] R. Escribano *et al.*, *Phys. Lett.* **B444**, 397 (1998).

[30] P.C. de Hollanda *et al.*, *Phys. Rev.* **D60**, 093010 (2000).

[31] H.H. Chen, *Phys. Rev. Lett.* **55**, 1534 (1985); A.B. McDonald, Neutrino98, *Nucl. Phys. B (Proc. Suppl)* **B77**, 43 (1999).

[32] L. Oberauer, Neutrino98, *Nucl. Phys. B (Proc. Suppl)* **B77**, 48 (1999.

[33] A. Suzuki, Neutrino98, *Nucl. Phys. B (Proc. Suppl)* **B77**, 171 (1999).

[34] A.Suzuki *et al.*, submitted to *Nucl. Instrum. Methods A.*, `hep-ex/0004024`.

[35] A. Para, *Acta Phys. Pol.* **B31**, 1313 (2000).

[36] A. Rubbia, *Acta Phys. Pol.* **B31**, 1287 (2000).

[37] G. Iovane, DARK98-Second International Conference on Dark Matter in Astro and Particle Physics, Heidelberg, Germany, `hep-ex/9812015`.